

The Age-Metallicity Degeneracy in the Dwarf Spheroidal Carina as Seen by FLAMES

Andreas Koch¹
 Eva K. Grebel¹
 Rosemary F. G. Wyse²
 Jan T. Kleyna³
 Mark I. Wilkinson⁴
 Daniel R. Harbeck⁵
 Gerard F. Gilmore⁴
 N. Wyn Evans⁴

¹ Astronomical Institute of the University of Basel, Department of Physics and Astronomy, Binningen, Switzerland

² The Johns Hopkins University, Baltimore, USA

³ Institute for Astronomy, Honolulu, USA

⁴ Institute of Astronomy, Cambridge University, United Kingdom

⁵ Department of Astronomy, University of Wisconsin, Madison, USA

The Carina dwarf spheroidal galaxy is the only one of this type to show clearly episodic star formation separated by long pauses. Still its Red Giant Branch is remarkably narrow. Our medium-resolution spectroscopy of 437 Red Giants in this galactic satellite with FLAMES reveals a full range of metallicities from ~ -3.0 up to ~ 0.0 dex. There also appears to be a mild radial gradient in that more metal-rich populations are more centrally concentrated, matching a similar trend in ages with an increasing fraction of intermediate-age stars in the centre (Harbeck et al. 2001). Complemented by the colours of the more metal-rich stars, this suggests that Carina exhibits an age-metallicity relation. We address the star formation in this intriguing galaxy by also pursuing its age-metallicity degeneracy, resulting in a narrow Red Giant Branch despite the considerable spread in metallicity and wide range of ages, and applying basic models of chemical evolution.

Dwarf spheroidal galaxies (dSphs) are the least luminous, least massive galaxies known. Most of them are found within 300 kpc around more massive galaxies. DSphs are gas-deficient and are typically dominated by old (> 10 Gyrs) or intermediate-age populations (1–10 Gyrs). All dSphs studied in sufficient detail have been found to contain ancient populations that are indistinguishable in age from

the oldest populations in the Milky Way (Grebel and Gallagher 2004). While their detailed star-formation histories (SFHs) vary from galaxy to galaxy, dSphs exhibit a trend of increasing luminosity with increasing mean metallicity (e.g., Grebel, Gallagher, and Harbeck 2003). DSphs usually show fairly continuous star formation (SF) with some amplitude variations. Younger and/or more metal-rich populations are more centrally concentrated, indicating longer-lasting SF episodes in the centres of the dSphs' shallow potential wells (Harbeck et al. 2001).

DSphs are enigmatic objects. Their past extended SF histories contrast with their present, puzzling lack of gas. It is still under debate whether they are dark matter dominated and how much dark matter they contain. While they clearly interact with more massive galaxies, their importance as cosmological building blocks remains unclear. Not only do cosmological models predict two orders of magnitude more 'dark matter halos' than the observed number of low-mass dSphs (e.g., Moore et al. 1999), but also the element abundance ratios in the galactic halo differ from those measured in dSphs (e.g., Shetrone, Côté, and Sargent 2001).

Our current knowledge of the detailed evolutionary history of nearby dwarf galaxies is mainly based on photometry, occasionally supplemented by rather sparse spectroscopic information. But spectroscopy is of paramount importance since it permits us to break the age-metallicity degeneracy that plagues purely photometric colour-magnitude-diagram analyses. The information from independent spectroscopic metallicity determinations for individual stars removes this ambiguity from subsequent photometric determinations of the SF history.

In the gas-deficient dSphs, our primary sources of metallicity information are Red Giants, which are now easily accessible for ground-based 8- to 10-m-class telescopes. Thus, we may ultimately be able to derive detailed evolutionary histories by using the VLT with its powerful multi-object spectroscopy facility FLAMES. Moreover, velocities can be extracted from such spectra, permitting membership and kinematic analyses.

Our VLT Large Programme (171.B-0520, PI: Gilmore) aims at doing just that: We wish to (1) constrain the chemical evolution of dSphs and to (2) measure the size and extent of the dark-matter halos of dSphs. One of our prime targets is the galactic dSph companion Carina at a distance of about 94 kpc from the Milky Way. Here we present first results of our abundance analysis of Carina (see also Koch et al. 2006). A detailed kinematic analysis is in preparation (Wilkinson et al. 2006).

The dwarf galaxy Carina

Carina stands out among the dSphs in the Local Group because of its unusual, episodic star-formation history (e.g., Smecker-Hane et al. 1994). In no other dSph has clear evidence for well-separated episodes of star formation been found. Carina may have experienced at least four episodes of star formation, one possibly as recently as 0.6 Gyr ago (Monelli et al. 2003). The dominant episodes occurred approximately 2, 3 to 6, and 11 to 13 Gyrs ago. Their distinct main-sequence turn-offs all connect to the same narrow Red Giant Branch with an estimated mean metallicity of $[\text{Fe}/\text{H}] \sim -1.99$ dex and a spread of about 0.08 dex (Smecker-Hane et al. 1999). Smecker-Hane et al. (1999) argue that the narrow Red Giant Branch of Carina results from an age-metallicity conspiracy in the sense that more metal-rich, but younger stars come to lie at the same location in the colour-magnitude plane as older, metal-poor stars. Based on a photometric study, Rizzi et al. (2003) suggest that the narrow Red Giant Branch is a consequence of the contribution of the dominant intermediate-age star-formation episode, while the contribution of the ancient episode is almost negligible, which cannot be rejected as a plausible cause, unless reliable spectroscopic age estimates are available.

These findings underline the highly complex star-formation history of Carina. There is not yet a satisfactory explanation of why Carina would have experienced episodic SF, and why its evolution was so different from that of other dSphs. Was Carina's SF activity triggered by interactions? Did this dSph manage to repeat-

edly accrete potentially unenriched gas?
Did feedback halt its SF periodically?

Red Giant spectroscopy

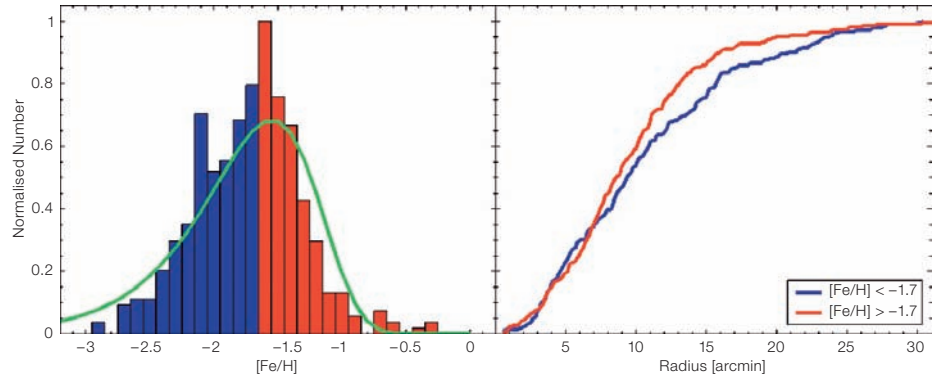
Determinations of accurate spectroscopic abundances require a well-calibrated and widely applicable reference scale. The infrared lines of the singly ionised calcium ion at 849.8, 854.2, 866.2 nm have become one of the spectral features of choice, since these Ca triplet (CaT) lines can be relatively easily distinguished as the strongest absorption lines in the near infrared regime of Red Giant Branch (RGB) spectra, where true Fe absorption features become increasingly weaker at intermediate resolution. Cole et al. (2004) extended the CaT calibration to ages as young as 2.5 Gyrs, providing a good match to the expected dominant populations in Carina.

We observed these three lines in 1257 Red Giant candidates in Carina in the framework of our ESO Large Programme. Our targets are distributed across five fields in the galaxy to cover most of Carina's area, but also reach beyond its nominal tidal radius. The observations were carried out in 22 nights spread over two semesters in 2003 and 2004 using FLAMES/GIRAFFE in MEDUSA 'low-resolution' mode ($R = 6500$) and centred at the near-infrared CaT (~ 850 nm).

In addition, more than 80 Red Giant candidates in four calibration globular clusters were observed in order to permit us to place our CaT measurements on a scale of known reference metallicities (Rutledge et al. 1997; Carretta and Gratton 1997). These clusters range in metallicity from approximately -1.1 dex to -2 dex in $[\text{Fe}/\text{H}]$.

We selected our targets covering three magnitudes in brightness from the tip of the RGB downward. Since we selected stars across the full width of the RGB (approximately 0.2 mag in B-V), we circumvented any bias with respect to metallicity or age, and still could ensure the inclusion of potential extremely metal-poor and metal-rich giants. Our radial-velocity measurements led to the rejection of about 60% of the targeted stars as Galactic foreground contamination, leaving

Figure 1: Left Panel: Metallicity distribution of Red Giants derived from CaT spectroscopy in Carina, where the colour-shading illustrates the separation used in the right panel. The green line illustrates a best-fit closed-box model. The right panel displays



us with a total number of 437 Red Giants around Carina's systemic velocity of 223.9 km s^{-1} .

Carina's wide metallicity range

The distribution of the metallicities derived from our CaT spectroscopy is shown in Figure 1 (left). This metallicity distribution function (MDF) is peaked at a mean metallicity of -1.72 ± 0.01 dex, slightly higher than the previously derived mean spectroscopic metallicity of -1.99 ± 0.08 dex from a CaT sample of 52 RGB stars (Smecker-Hane et al. 1999). These former results are in reasonable agreement with our data if the quoted uncertainties and the widths of the distributions are taken into account.

The MDF appears remarkably broad. The entire distribution's *formal* full width at half maximum is 0.92 dex (1σ -width of 0.39 dex). The *full* metallicity range, on the other hand, covers approximately 3.0 dex, reflected in the extreme tails of the MDF, where we find stars with metallicities approaching -3 dex and near-solar metallicity, respectively, when extrapolating our calibration. Follow-up spectroscopy of these stars would be desirable to disclose the detailed chemical properties of these stars, which appear to be in part as metal-poor as the most metal-poor Red Giants found in other nearby dwarf galaxies (e.g., Shetrone et al. 2001). At the metal-rich end, a handful of them would be as metal-rich as the metal-rich population in the Sgr dSph (Bonifacio et al. 2004).

While part of the spread may be attributed to the usual measurement uncer-

cumulative spatial distributions of the metal-poor (blue) and metal-rich (red) components. The metal-rich stars clearly tend to concentrate towards the galaxy's centre.

tainties, to star-to-star variations in the actual Ca abundance (up to 0.2 dex), and calibration uncertainties, the spread in the metallicities seems to be influenced by the occurrence of several subpopulations with different peak metallicities.

Any MDF, as derived here, is rather insensitive to the details of the star-formation history. However, we have calibrated our CaT *metallicities* onto *iron* which in systems with extended star formation can have a significant contribution from long-lived stars through type Ia supernovae. Hence, one can have enrichment in Fe *without* accompanying SF. In the case of a SF history that consists of several SF episodes with long pauses in between, the Fe distribution can show 'gaps'. A Gaussian decomposition results in four underlying populations, which are preferred over a one-population model at the 98.1% level. However, one has to keep in mind that such a decomposition is a purely formal procedure, since SF events do not naturally produce Gaussian metallicity distributions.

Comparing our MDFs to simple chemical evolution models such as a closed-box model (see the green overplotted curve in the left panel of Figure 1) reveals a G dwarf problem at low metallicities: This model overpredicts the number of metal-poor stars. Also the pronounced metallicity peak of the MDF is not reproduced. Better fits may be obtained through the inclusion of infalling, pre-enriched gas and accounting for important outflows (Lanfranchi and Matteucci 2004). In this vein, one possible reason for the repeated cessation and onset of the SF episodes in Carina is the re-accretion of previously blown-out material. More de-

tailed chemical modeling to quantify the dominant processes is in preparation (Wyse et al., in prep.).

An age-metallicity relation?

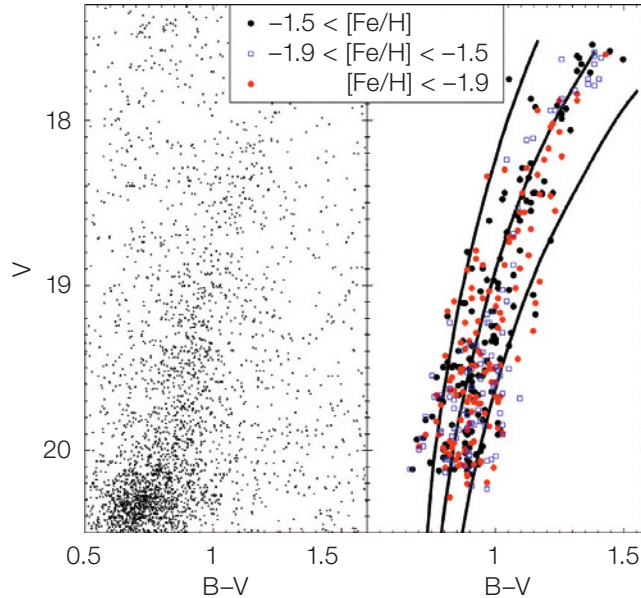
The (lack of a) relation between the colour of our targets and their metallicity is demonstrated in Figure 2 (right panel). In a population with little age spread, metal-poor stars would have blue colours and metal-rich ones would appear redder. This is indicated by three isochrones with metallicities, which span a similar range to those found in Carina and an age of its oldest population. In fact, there is no clear correlation with the data points. Obviously one cannot derive the metallicity of an individual star from its colour and magnitude on the RGB when dealing with mixed-age populations as in Carina. Our data thus confirm earlier suggestions that Carina shows an age-metallicity degeneracy in the sense that higher metallicities counteract the effects of younger ages. This conspiracy in turn leads to the observed narrow RGB.

Note that there are also quite a number of metal-poor stars ($[\text{Fe}/\text{H}] < -1.9$) present redwards of the most metal-rich isochrone. Each of the physical systems, for which such isochrones apply, have a Red Giant Branch of a finite width, despite the underlying ‘fixed’ metallicity. This becomes more pronounced towards the lower part of the RGB, where the different isochrones will lie closer together, and lead to a progressive overlap of the respective branches. That is, for any star of a given metallicity and age, one will inevitably end up with a large spread in colours. Bearing this in mind and accounting for photometric uncertainties, these effects will have a larger impact than the uncertainties in metallicities, and can account for the increased scatter in the colour-magnitude diagrams.

We also found a higher concentration of metal-rich, presumably intermediate-age stars towards the inner regions of the galaxy as compared to more metal-poor stars – indicated in the cumulative plot of the stars’ galactocentric radii (Figure 1, right). Metal-poor stars are, however, detected throughout the entire galaxy. This trend matches the observed population

Figure 2: Left panel: Carina’s narrow Red Giant branch (from EIS photometry). Also visible at the lower left is the prominent intermediate-age red clump. The right panel shows confirmed member stars, colour coded by their metallicity. Also

shown (black lines) are sets of Yonsei-Yale isochrones with an age of 12.6 Gyrs and (left to right) $[\text{Fe}/\text{H}] = -2.3$, $[\text{Fe}/\text{H}] = -1.7$ and $[\text{Fe}/\text{H}] = -1.3$, which illustrate the effects of Carina’s prominent age-metallicity degeneracy.



gradient in terms of a central concentration of intermediate-age stars in Carina (Harbeck et al. 2001). This supports the idea that the more metal-rich stars are also the younger ones. A possible reason for such a gradient can be stronger dissipation of the more metal-enriched gas. It may as well indicate that the material at disposal for SF is more easily retained at the centre of the galaxy’s shallow potential well.

Outlook

Carina is the only dSph known to have undergone distinct, well-separated episodic star formation. The dominant episodes of star formation took place at intermediate ages. It is not yet understood what caused the repeated cessation and delayed re-start of star formation in this enigmatic dSph.

We have compiled a large spectroscopic sample of CaT metallicities in Carina, which exceeds the previously largest published data set (Smecker-Hane et al. 1999) by more than a factor of eight. This will help us to disentangle its pronounced age-metallicity degeneracy and the galaxy’s age structure, since we can now in principle derive age estimates for our stars of known metallicity from finding the best-matched isochrone at that metallicity. Ultimate age distributions and

age-metallicity relations can additionally be well derived from turn-off stars, provided that the photometry is at a sufficient level of accuracy. Such an analysis, complemented by high-resolution spectroscopy, is currently in progress. A second article, giving an overview of the whole project, will be published in the June issue of *The Messenger*.

References

- Bonifacio, P. et al. 2004, *A&A* 414, 503
- Carretta, E. and Gratton, R. 1997, *A&AS* 121, 95
- Cole, A. et al. 2004, *MNRAS*, 347, 367
- Grebel, E. K., Gallagher, J. S., and Harbeck, D. 2003, *AJ* 125, 1926
- Grebel, E. K. and Gallagher, J. S. 2004, *ApJ* 610, L89
- Harbeck, D. et al. 2001, *AJ* 122, 3092
- Koch, A. et al. 2005, *AJ* 131, 895
- Lanfranchi, G. A. and Matteucci, F. 2004, *MNRAS* 351, 1338
- Monelli, M. et al. 2005, *AJ* 126, 218
- Moore, B. et al. 1999, *ApJ* 542, L19
- Rizzi, L. et al. 2003, *ApJ* 589, L85
- Rutledge, G., Hesser, J. E., and Stetson, P. B. 1997, *PASP* 109, 907
- Shetrone, M. D., Côté, P., and Sargent, W. L. W. 2001, *ApJ* 548, 592
- Smecker-Hane, T. A. et al. 1994, *AJ* 108, 507
- Smecker-Hane, T. A. et al. 1999, *ASP Conf. Ser.* 192, 159